Observation of Low Frequency MHD Mode Driven by Energetic Particles in Large Helical Device Plasmas with Strong Interchange Mode Activities*)

Wei CHEN[1)], Mitsutaka ISOBE[1,2)], Kazuo TOI[1,3)], Kunihiro OGAWA[3)], Xiaodi DU[2)], Masaki OSAKABE[1)], Satoshi OHDACHI[1,2)] and LHD Experiment Group

[1)]*National Institute for Fusion Science, 322-6 Oroshi-cho, Toki 509-5292, Japan*
[2)]*Department of Fusion Science, The Graduate University for Advanced Studies, 322-6 Oroshi-cho, Toki 509-5292, Japan*
[3)]*Department of Energy Science and Engineering, Nagoya University, Furo-cho, Nagoya 464-8603, Japan*

(Received 12 December 2011 / Accepted 25 April 2012)

The beta-induced Alfvén eigenmode (BAE) like modes during strong interchange mode, whose mode-numbers are $m/n = 2/1$, have been recently observed for the first time in Large Helical Device (LHD). The first harmonic frequencies of these oscillations range from 30 to 70 kHz, much lower than the toroidal-Alfvén-eigenmode (TAE) frequency, and are provided with the same order of the low-frequency gap induced by finite beta effects. The magnetic fluctuation spectrogram indicates that the BAEs often occur in pairs, and their mode-numbers are $m/n = 2/1$ and $-2/-1$. The analysis reveals that the modes propagate poloidally and toroidally in opposite directions, and form standing-wave structures in interchange-mode rest frame. The frequencies of the pair mode are associated with the T_e/T_i ratio, and the frequency difference of the pair modes is determined by the frequency of interchange mode. The new finding shed light on the underlying physics mechanism for the excitation of the low frequency Alfvénic fluctuation.

Keywords: LHD, BAE, interchange mode, dispersion relation, mode idenfication

DOI: 10.1585/pfr.7.2402079

1. Inroduction

The low-frequency Alfvénic and acoustic fluctuations driven by fast particles, such as beta-induced Alfvén eigenmode (BAE), Alfvén cascade (AC, also called RSAE), energetic-particle mode (EPM) and geodesic acoustic mode (GAM), are presently of considerable interest in the present-day fusion and future burning plasmas. The low-frequency waves can significantly affect the plasma performance, and induce the large fast particle losses and reduce the plasma self-heating, which are potentially harmful in future fusion reactors. The instabilities can play a key role in turbulence and anomalous transport regulation, especially, while there is significant fraction of high energy particles in plasma. They can be used as energy channels to transfer the fusion-born-alpha-particle energy to the thermonuclear plasma [1]. Their MHD spectroscopy can give some valuable information about the plasma equilibrium, e.g. safety factor and ion temperature [2].

The BAEs were observed and investigated under different conditions in tokamak plasma, including that driven by fast ions on DIII-D [3], energetic electrons on HL-2A [4], and large magnetic islands on FTU [5], HL-2A [6] and TEXTOR [7]. Recently, the BAEs have also been reported during a sawtooth cycle with fast ions ASDEX-U [8], Tore-Supra [9] and HL-2A [10]. The BAEs occur in the low-frequency kinetic thermal ion (KTI) gap in the shear Alfvén wave (SAW) continuous spectrum [11]. The stability mechanism of BAE is more complex than toroidal Alfvén eigenmodes (TAE) because the many kinetic effects play crucial roles in the mode excitation, saturation or damping [12–14]. The effects include the ion diamagnetic drift, thermal ion compression, finite Larmor radius (FLR), finite orbit width (FOW), and energetic-particle effects, and so on.

The paper is organized as follows. Section II introduces the experimental conditions. Section III addresses the excitation of BAE-like mode during strong interchange (IC) modes. The generalizedfishbone-like dispersionrelation (GFLDR) and identification of BAE-like modes are present in section IV. The summary and discussion are given in the last section.

2. Experimental Apparatus and Conditions

LHD is a large superconducting helical device with toroidal period number $M = 10$ and multipolarity $l = 2$. The major radius and minor radius are $R_0 = 3.9$ m and $a \sim 0.6$ m, respectively [15]. The LHD is equipped with two

author's e-mail: chenw@swip.ac.cn
*) This article is based on the presentation at the 21st International Toki Conference (ITC21).

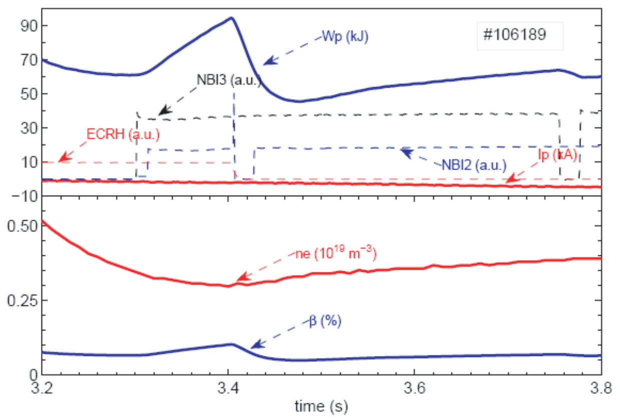

Fig. 1 Time traces of plasma parameters, NBI and ECRH of shot #106189. Stored energy W_p, plasma current I_p, line averaged electron density n_e and plasma beta β.

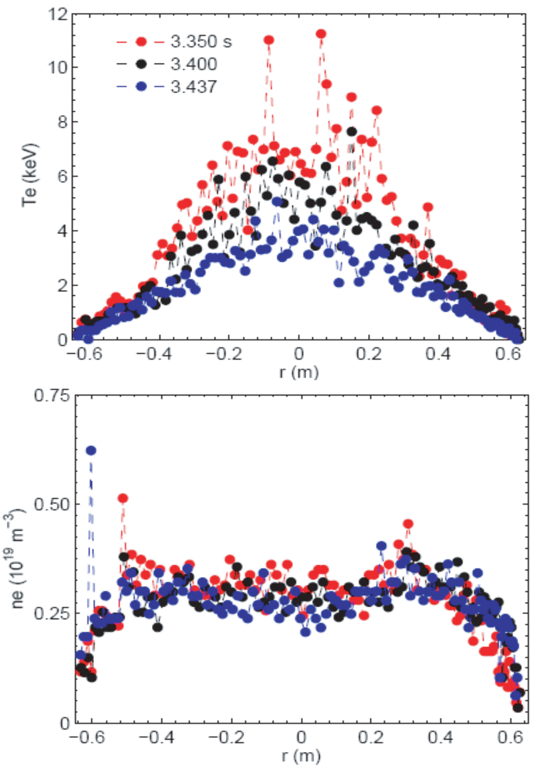

Fig. 2 Electron temperature and density profiles measured by Thomson scattering (TS) at different times for shot #106189.

positive-ion-source-based neutral beam (P-NB) injectors ($P_{nb}/E_b \sim 6$ MW/40 keV) and with three negative-ion-source-based neutral beam (N-NB) injectors ($P_{nb}/E_b \sim 5$ MW/180 keV). The P-NB is almost perpendicular to the magnetic field line. The N-NB1 and N-NB3 are all tangentially injected in the counterclockwise (CCW) direction as seen from the top of LHD, but the N-NB2 is injected oppositely, i.e. in the clockwise (CW) direction. Meanwhile, the ECRH system with three 77 GHz / 1 MW and one 84 GHz / 0.3 MW gyrotrons has been built up and successfully used on LHD. Combining these features with the NBI and ECRH systems, LHD is an excellent fusion device for exploring and studying energetic-particle physics. The P-NBs create helically trapped energetic-ion, and the N-NBs produce the circulating energetic-ions, and the ECRH induces the production of superthermal electrons. These energetic-particles can destabilize the AEs and EPMs. The typical MHD activities are observed using a set of Mirnov probes (toroidal 6ch and poloidal 13 ch) localized the vessel of LHD, and all magnetic fluctuations are measured by a Nyquist frequency 250 kHz or 500 kHz.

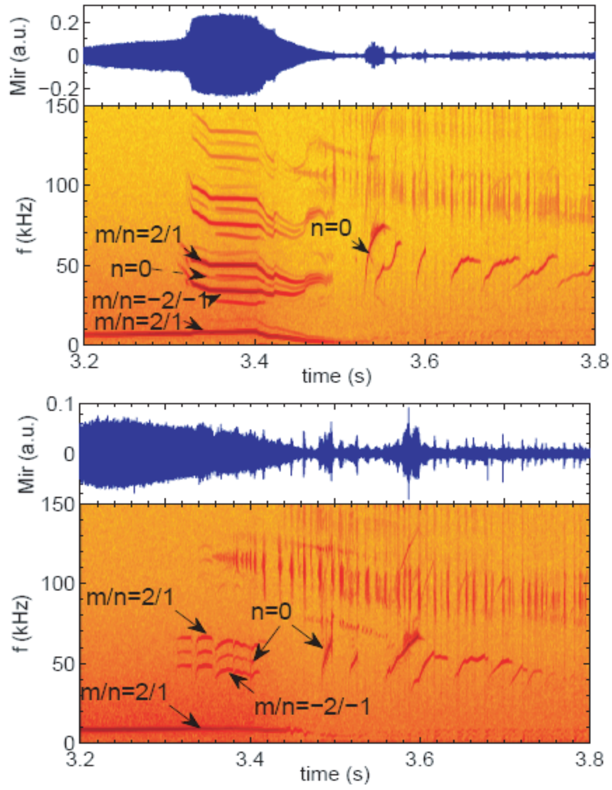

Fig. 3 Magnetic probe signal with IC mode and BAE-like modes, and corresponding to spectrogram. (a) Shot #106189 (top) and (b) Shot#106185 (bottom).

3. Excitation of BAE-like Modes

During strong IC mode, the BAE-like modes have been recently observed for the first time in LHD. Being BAE-like activities, the discharge waveforms and plasma profiles have been shown in Fig. 1 and Fig. 2. In this discharge, the initial magnetic axis position $R_{ax} = 3.75$ m and the toroidal field $B_t = 2.64$ T. The plasma current is generated by the N-NB2 ($P_{nb}/E_b \sim 2.3$ MW/180 keV), N-NB3 ($P_{nb}/E_b \sim 2.5$ MW/180 keV) and the ECRH (77 GHz / 2.05 MW & 84 GHz / 0.16 MW) launched into the plasma from $t = 3.0$-3.4 s.

The spectrograms of Mirnov-coil signals have revealed the existence of many kind MHD instabilities in Fig. 3. From Fig. 3 (a), it is seen that the lower frequency ($f < 10$ kHz) MHD activity is an interchange (IC) mode with mode-number $m/n = 2/1$ during $t = 3.20$-3.54 s,

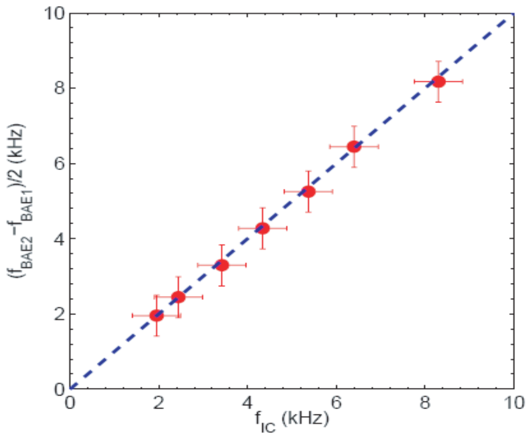

Fig. 4 Half frequency difference $\Delta f = (f_{\mathrm{BAE2}} - f_{\mathrm{BAE1}})/2$ of two-branch BAE-like modes versus the IC mode frequency f_{IC}. Marker points indicate experimental data. The dash curve shows the linear-fit result.

and some other interesting high frequency instabilities (HFIs) (1st harmonics, f = 25-70 kHz) and their harmonics are also excited during t = 3.30-3.50 s. The fundamental frequencies of modes are all lower than TAE ones ($f_{\mathrm{TAE}} \approx 350$ kHz for the hydrogen plasma with $B_{\mathrm{t}} = 2.64$ T, $n_{\mathrm{e}} = 0.3 \times 10^{19}\,\mathrm{m}^{-3}$, $R = 3.75$ m and $q = 2$ on LHD). The detailed mode-number analysis and calculation analysis (see sec.3.3) suggest that the primary HFIs are two branch BAEs with $m/n = 2/1$ & $-2/-1$ and GAM with $n = 0$, respectively. From Fig. 3 (a), it is also shown that the BAE-like modes are driven while the IC mode amplitude is large during t = 3.30-3.50 s, and there exists GAM with consant frequency. To the contrary, the BAE-like modes are stable while the IC mode is very weak or nothingness during t = 3.50-3.80 s, and the GAM frequency shifts upward, and $O(\min(f_{\mathrm{GAM}})) = O(f_{\mathrm{BAE\text{-}like}})$ (here 'O' indicates the frequency order). The HFIs are provided with the same order of the low-frequency gap induced by finite beta effects. The BAE-like mode frequencies decrease as the electron temperatures measured by Thomson scattering (TS) drop at three different times (see Fig. 2 and Fig. 3), it means that the mode frequencies depend on the plasma temperatures.

The frequency difference Δf between the two-branch BAE modes is exactly twice the fundamental frequency f_{IC} of the IC modes, namely, $\Delta f = f_{\mathrm{BAE2}} - f_{\mathrm{BAE1}} = 2 f_{\mathrm{IC}}$ (see Fig. 4). Here, it must be pointed out that all the observed data satisfy the relation, $\Delta f = 2 f_{\mathrm{IC}}$. It means that that the BAE-like modes propagate poloidally and toroidally in opposite directions, and form standing-wave structures in IC mode rest frame and the frequency difference of them is determined by the frequency of IC mode. These experimental results indicate that this phenomenon is very similar with that of BAE during strong tearing mode in tokamak plasma [5–7], but the BAE frequencies do not completely depend on the intensity of interchange mode on LHD, and the fast particle effects maybe also important (see Fig. 3).

4. GFLDR and Identification of BAE-like Modes

The BAE excitation can be described using the generalized fishbone-like dispersion relation (GFLDR) [13, 14, 16]. The GFLDR developed by L. Chen & F. Zonca is used to study plasma dynamics with the frequency range from kinetic ballooning mode (KBM)/BAE to TAE.

The GFLDR can be given by

$$-i\Lambda(\omega) + \delta\hat{W}_f + \delta\hat{W}_k = 0 \tag{1}$$

Where $i\Lambda(\omega)$ is the inertial layer contribution due to thermal ions, while $\delta\hat{W}_f$ and $\delta\hat{W}_k$ come from fluid MHD and energetic particle contributions in the regular ideal regions.

For BAE

$$\begin{aligned}\Lambda^2 = {} & \frac{\omega^2}{\omega_A^2}\left(1 - \frac{\omega_{*\mathrm{pi}}}{\omega}\right) \\ & + q^2\frac{\omega\omega_{\mathrm{ti}}}{\omega_A^2}\left[\left(1 - \frac{\omega_{*\mathrm{ni}}}{\omega}\right)F - \frac{\omega_{*\mathrm{Ti}}}{\omega}G - \frac{N^2}{D}\right]\end{aligned} \tag{2}$$

$$\begin{aligned}\omega_{*\mathrm{ni}} &= (T_{\mathrm{i}}c/eB)(\vec{k}\times\vec{b})\cdot\nabla n_{\mathrm{i}}/n_{\mathrm{i}} \\ \omega_{*\mathrm{Ti}} &= (T_{\mathrm{i}}c/eB)(\vec{k}\times\vec{b})\cdot\nabla T_{\mathrm{i}}/T_{\mathrm{i}} \\ \omega_{*\mathrm{pi}} &= \omega_{*\mathrm{ni}} + \omega_{*\mathrm{Ti}} = \omega_{*\mathrm{Ti}}(1 + 1/\eta), \\ \eta &= \nabla \ln T_{\mathrm{i}}/\nabla \ln n_{\mathrm{i}}\end{aligned}$$

Here $\omega_{\mathrm{ti}} = (2T_{\mathrm{i}}/m_{\mathrm{i}})^{1/2}/qR$ is the ion transit frequency, and the functions in eq.(2), $F(x)$, $G(x)$, $N(x)$ and $D(x)$ are defined as,

$$\begin{aligned}F(x) &= x(x^2 + 3/2) + (x^4 + x^2 + 1/2)Z(x), \\ G(x) &= x(x^4 + x^2 + 2) + (x^6 + x^4/2 + x^2 + 3/4)Z(x), \\ N(x) &= (1 - \omega_{*\mathrm{ni}}/\omega)[x + (1/2 + x^2)Z(x)] \\ &\quad -(\omega_{*\mathrm{Ti}}/\omega)[x(1/2 + x^2) + (1/4 + x^4)Z(x)]' \\ D(x) &= (1/x)(1 + \tau) + (1 - \omega_{*\mathrm{ni}}/\omega)Z(x) \\ &\quad -(\omega_{*\mathrm{Ti}}/\omega)[x + (x^2 - 1/2)Z(x)]\ ,\end{aligned}$$

with $x = \omega/\omega_{\mathrm{ti}}$, $\tau \equiv T_{\mathrm{e}}/T_{\mathrm{i}}$ and $Z(x) = \pi^{-1/2}\int_{-\infty}^{+\infty} e^{-y^2}/(y - x)\mathrm{d}y$ the plasma dispersion function.

We solved the GFLDR to identify the modes with the BAE modes on LHD near marginal stability ($\Lambda = 0$). The BAE frequency depends on local thermal ion temperature, ratio of $T_{\mathrm{e}}/T_{\mathrm{i}}$, and diamagnetic frequency. In the 106189 discharge, the plasma temperature and density profiles are shown in Fig. 2. On the basis of experimental measurements and assumptions, we have $B = 2.64$ T, $r \approx 0.30$ m, $m_{\mathrm{i}} = 1.5$, $n_{\mathrm{e}} = n_{\mathrm{i}}$, $\nabla \ln T_{\mathrm{i}} = -4.0/\tau$, and $\nabla \ln n_{\mathrm{i}} = 0$ at the $q = 2$ surface. We obtain $k_\theta \approx m \cdot 3.3\,\mathrm{m}^{-1}$, and $\omega_{*\mathrm{pi}}/2\pi \approx mT_{\mathrm{e}}/\tau \cdot 1.61$ kHz. According to the parameters and assuming $\Lambda = 0$, the solutions of Eq.2 have been present in Fig. 5. Using the experimental data at $t = 3.4$ s, the ion diamagnetic frequency is $\omega_{*\mathrm{pi}}/2\pi \approx 10.3/\tau$ kHz at the $q = 2$ surface with $T_{\mathrm{e}}|_{q=2} \approx 3.2$ keV. The observed frequency is around $f = (f_{\mathrm{BAE1}} + f_{\mathrm{BAE2}})/2 \approx 43$ kHz, while the frequency of the BAE accumulation point is around $f \approx 40$ kHz for $\tau = 2$ and $f \approx 48$ kHz for $\tau = 1$. It

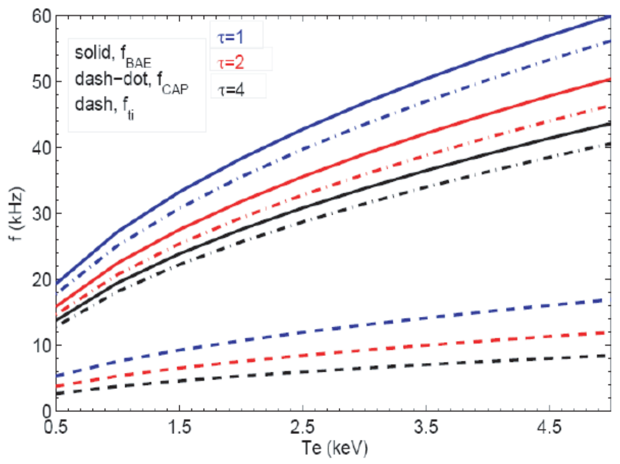

Fig. 5 BAE accumulation point and ion transit frequencies versus electron temperature at $q = 2$ surface. Note that $f_{\rm BAE}$ is from eq. (2) in the case of $\Lambda = 0$, $f_{\rm CAP} = (7/4 + T_{\rm e}/T_{\rm i})^{1/2} q\omega_{\rm ti}/2\pi$ and $f_{\rm ti} = (2T_{\rm i}/m_{\rm i})^{1/2}/2\pi qR$.

is obvious that the observed frequencies are close to theoretical prediction based on the GFLDR. This result, along with the experimental evidence reported above, supports that the modes are the BAE instabilities. However, the observed frequencies are more than that predicted by the GFLDR at $t = 3.31$ s for shot #106189, i.e. the frequency mismatch exists, so they are called BAE-like modes. In addition, the GAM and BAE-like modes can be observed simultaneously under same discharge parameter conditions. Figure 3 present $O(f_{\rm GAM}) \approx O(f_{\rm BAE\text{-}like})$ due to their adjacent localized positions during $t = 3.30$-3.50 s for shot #106189 and $t = 3.30$-3.40 for shot #106185. It also suggests further that these modes are the BAE-like activities.

5. Summary and Discussion

In the present paper, the BAE-like modes during strong IC mode, whose mode-numbers are $m/n = 2/1$, have been recently observed for the first time on LHD. The first harmonic frequencies of these oscillations range from 30 to 70 kHz on LHD, much lower than the TAE frequency. The magnetic fluctuation spectrogram indicates that the BAE-like modes often occur in pairs, and their mode-numbers are $m/n = 2/1$ and $-2/-1$. The analysis reveals that the modes propagate poloidally and toroidally in opposite directions, and form standing-wave structures in IC mode rest frame. The mode frequencies are associated with the $T_{\rm e}/T_{\rm i}$ ratio, and the frequency difference of the pair modes is determined by the frequency of IC mode. The observed mode features agree with the predictions of the GFLDR, qualitatively, but the frequency mismatch exists, sometimes. The experimental results indicate that this phenomenon is very similar with that of BAE during strong tearing mode in tokamak plasma, but the BAE frequencies do not completely depend on the intensity of IC mode. Comparing with the tearing mode, although the free energy, which drives the IC mode, is different, the steepen pressure gradients at the vicinity of resonant surface both potentially excite the type of BAE-like instability. The new findings give a deep insight into the underlying physics mechanism for the excitation of the low frequency Alfvénic fluctuation.

Recently, the two new theories are proposed for interpreting corresponding experimental phenomena. A theory indicates that the poloidal gradient of the equilibrium distribution function of thermal ions, induced by the combined effect of the geodesic curvature and magnetic island, which can provide the source of free energy for the excitation of the BAE [17]. However, noting here that we do not consider the effects of magnetic island because the island-width is still not assessed up to date. Another theory is that, inside a magnetic island, there is a continuous spectrum very similar to that of tokamak plasmas [18]. The strong eccentricity of the island cross section induces a gap formation. There exists a discrete eigenmode in the gap, and the mode frequency depends on the magnetic island size. But this theory cannot explain the experimental results completely. The comparison result indicates that the theoretical frequencies are larger than the experimental ones [19]. Further works need to be done, such as mode-structure and fast-particle-loss measurements, etc.

Acknowledgements

The author (C.W.) is very grateful to the LHD Group, and thanks Prof. L. Chen and Dr. F. Zonca for their teaching me many theories in the past years.

[1] A.F. Fasoli *et al.*, Nucl. Fusion **47**, S264 (2007).
[2] A.F. Fasoli *et al.*, Plasma Phys. Control. Fusion **44**, B159 (2002).
[3] W.W. Heidbrink *et al.*, Phys. Rev. Lett. **71**, 855 (1993).
[4] W. Chen *et al.*, Phys. Rev. Lett. **105**, 185004 (2010).
[5] P. Buratti *et al.*, Nucl. Fusion **45**, 1446 (2005).
[6] W. Chen *et al.*, J. Phys. Soc. Jpn. **79**, 044501 (2010).
[7] O. Zimmermann *et al.*, Proc. 32nd EPS Conf. on PPCF, P4.059 (2005).
[8] P. Lauber *et al.*, Plasma Phys. Control. Fusion **51**, 124009 (2009).
[9] C. Nguyen *et al.*, Plasma Phys. Control. Fusion **51**, 095002 (2009).
[10] W. Chen *et al.*, Nucl Fusion **51**, 063010 (2011).
[11] L. Chen and F. Zonca, Nucl. Fusion **47**, S727 (2007).
[12] F. Zonca *et al.*, Plasma Phys. Control. Fusion **38**, 2011 (1996).
[13] F. Zonca *et al.*, Plasma Phys. Control. Fusion **40**, 2009 (1998).
[14] F. Zonca *et al.*, Plasma Phys. Control. Fusion **48**, B15 (2006).
[15] M. Isobe *et al.*, Contrib. Plasma Phys. **50**, 540 (2010).
[16] F. Zonca *et al.*, Nucl. Fusion **49**, 085009 (2009).
[17] V.S. Marchenko and S.N. Reznik, Nucl. Fusion **49**, 022002 (2009).
[18] A. Biancalani *et al.*, Phys. Rev. Lett. **105**, 095002 (2010).
[19] A. Botrugno *et al.*, Proc. 37th EPS Conf. on PPCF, P4.110 (2010).